Earth and Planetary Science Letters 400 (2014) 302–312

Contents lists available at ScienceDirect

Earth and Planetary Science Letters

www.elsevier.com/locate/epsl

Demise of the rapid-field-change hypothesis at Steens Mountain: The crucial role of continuous thermal demagnetization

Robert S. Coe[a,*], Nicholas A. Jarboe[b], Maxime Le Goff[c], Nikolai Petersen[d]

[a] Earth and Planetary Sciences Department, University of California, Santa Cruz, CA 95064, USA
[b] Geosciences Research Division, Scripps Institution of Oceanography, La Jolla, CA, USA
[c] Équipe de Paléomagnétisme, Institut de Physique du Globe, Paris, France
[d] Department of Earth and Environmental Sciences, Ludwig Maximilians University, Munich, Germany

ARTICLE INFO

Article history:
Received 8 December 2013
Received in revised form 16 May 2014
Accepted 21 May 2014
Available online 16 June 2014
Editor: J. Brodholt

Keywords:
Earth's magnetic field
Steens Mountain reversal
rapid field change
continuous thermal demagnetization
viscous remanent magnetization
Triaxe vibrating sample magnetometer

ABSTRACT

Rapid continuous thermal demagnetization in a Triaxe vibrating sample magnetometer disproves an earlier hypothesis that an episode of extraordinarily fast field change is recorded in the remanent magnetization of a single lava flow that cooled during a geomagnetic polarity reversal. The original evidence for this hypothesis was the distinctive pattern of variation in direction with vertical position after stepwise demagnetization to 500 °C, but continuous thermal demagnetization now proves that this flow actually carries consistent high-temperature remanence parallel to that of the flow immediately below. Why does continuous thermal demagnetization succeed when conventional thermal and alternating-field demagnetization fail to isolate this direction? Detailed investigation of the demagnetization trajectories and underlying rock-magnetic properties suggest that normal-polarity secondary remanent magnetization, acquired both at room temperature in today's polarity chron and during modest reheating in a normal field during cooling of the overlying flow, is responsible for the misleading pattern of directions. Alteration during ordinary thermal demagnetization evidently promotes the overprint to higher blocking temperatures so that it masks the primary component, whereas the rapid heating (∼40 °C/min) during continuous demagnetization is fast enough to demagnetize the normal overprint before this masking can happen.

1. Introduction: evolution of the rapid-field-change hypothesis

Almost fifty years ago Watkins (1965) discovered a paleomagnetic reversal transition zone in Steens Mountain lava flows in southeastern Oregon (Figure S-4a and 4b). These flows are now believed to be the earliest manifestation of Yellowstone hotspot flood-basalt volcanism, which started around 16.7 Ma and led soon thereafter to the massive outpouring of the Columbia River basalt lavas farther to the north (Hooper et al., 2002; Camp et al., 2013). Along the steep basin-and-range scarp that forms the east side of Steens Mountain hundreds of superposed basaltic flows are especially well exposed, and the paucity of interbedded material suggests that they were emplaced quite rapidly (Figure S-4c). The possibility of attaining a detailed volcanic record of field behavior during a polarity reversal attracted further paleomagnetic scrutiny, culminating in a benchmark directional record shown in Fig. 1a and b with 49 distinguishable directions, and almost as many paleointensities of the field (Mankinen et al., 1985; Prévot et al., 1985a, 1985b) from two well exposed sections A and B on the escarpment two kilometers apart. Section B is tied to A by multiple redundant flow directions where they overlap and extends the record below the bottom of A, which is interrupted by a fault. Within this detailed record, however, are three large gaps of ∼90° between one directional group and the next. These could represent an interlude in eruptive activity, but the absence of signs of an unusual hiatus between successive flows bounding the gaps suggested that instead the field might have changed very rapidly ('impulsively') at these times (Mankinen et al., 1985; Prévot et al., 1985b). At both the first and second gap this idea was reinforced by directional differences found in samples at varying vertical positions in a single flow at each of them that could have arisen if the field direction changed appreciably during the week or two that the flow took to cool and become magnetized.

These tantalizing results spurred detailed sampling from bottom to top of flows at the directional gaps. Results for these samples from flow B51 at the first gap were intriguing (Coe and Prévot, 1989). Careful thermal demagnetization revealed large variation in directions, both in individual samples and between samples, that were streaked out in a systematic manner. The direction of high-temperature remanence in B51 after demagnetization to 500 °C

* Corresponding author. Tel.: +1 831 459 2393; fax: +1 831 459 3074.
E-mail address: rcoe@pmc.ucsc.edu (R.S. Coe).

http://dx.doi.org/10.1016/j.epsl.2014.05.036

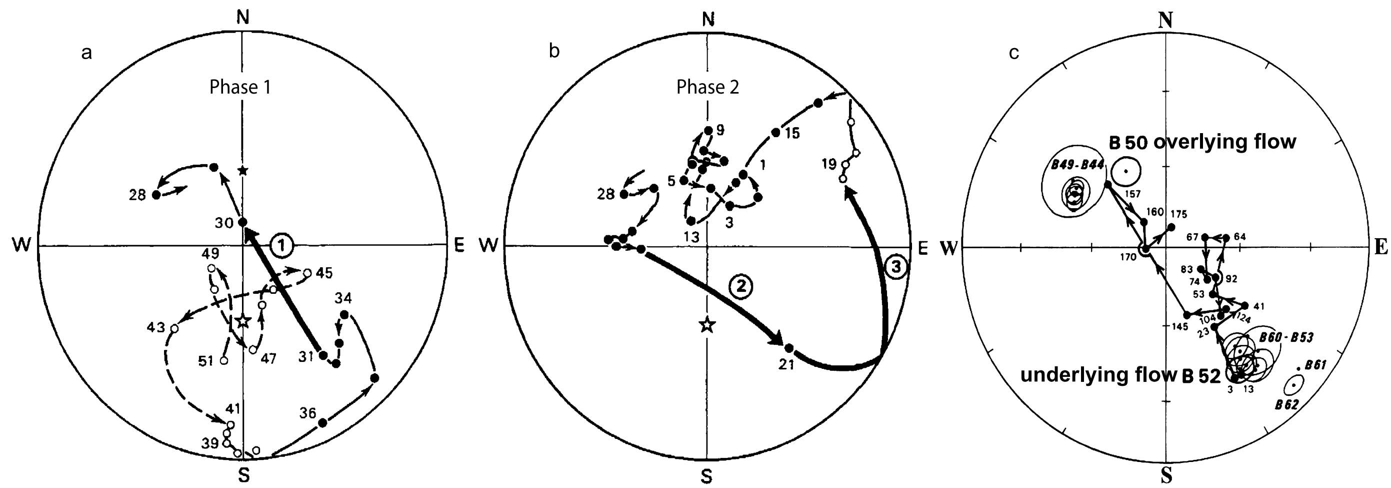

Fig. 1. The Steens Mountain reversal record as of 1989. (a and b) Variation in paleomagnetic field direction during the reversal recorded in superposed lava flows of Steens Mountain sections A and B, from the benchmark record of Mankinen et al. (1985). Note the three large gaps shown by thick black arrows. Each point on the equal-area projections represents a directional group (average direction of a group of superposed flows with indistinguishable directions), solid and open circles indicate downward and upward inclinations, respectively. Six reversed directions that were spliced into the original record from section C, 130 km to the southwest, are omitted. Adapted from Prévot et al. (1985b). (c) Variation in direction of flow B51 samples at the 500 °C thermal demagnetization step as a function of position found by Coe and Prévot (1989). Small numbers next to each direction indicate height in centimeters above the base of B51 for each sample. Shown as well are the mean directions and 95% uncertainty circles of the underlying flow B52 (plus the next lower ten flows) and the overlying flow B50 (plus the next six higher flows). Note that, contrary to an overprinting mechanism of simple baking by the overlying flow, (i) the trend of directions 3 to 67 cm above the base is not along a great circle between the B50 and B52 flow means and (ii) the directions 67–124 cm above the base move back towards the B52 direction.

varied systematically with height in this 1.9 m thick flow, trending from close to the underlying B52 direction at 3 to 13 cm above the base of flow B51 to a direction 60° away at 67 cm, returning to only 25° away at 104–124 cm, and then moving farther away again toward the overlying flow B50 direction for samples even higher in the section (Fig. 1c). Calculations show 53–73 cm above the base would be last to cool to 500 °C, so such variation in direction with position in the lower two-thirds of the flow could arise if the field changed direction while the flow was cooling and becoming magnetized, and the directions in the upper one-third of the flow are easily explained as thermal and chemical overprinting due to baking by the overlying flow. Although the implied rate of change of the field was extraordinarily high (∼300 nT/day) due to the rapidity with which such a thin flow would cool, at the time this hypothesis required less special pleading than others invoking undemonstrated rock-magnetic mechanisms (Coe and Prévot, 1989).

Detailed study of samples spanning flows at the second directional gap revealed similar smearing of paleomagnetic directions (Coe et al., 1995). For this study samples were taken 250 m from where suspicious within-flow directional variation was originally detected because the geometry of the cooling units was simpler and overall exposure better there. Indeed, directional results published later from the original locality were complex (Camps et al., 1995a), whereas at this section the high-temperature direction within the critical 1.3 m flow again moved systematically with distance from the base about 60° away from the direction of pre-gap flows toward the direction of post-gap flows and then back again, as shown in Figs. 2 and 3 in Coe et al. (1995). Assuming that the temperature of remanence unblocked during thermal demagnetization is essentially the same as when that remanence was acquired during primary cooling, a conductive cooling model reproduces the thermal data reasonably well (Camps et al., 1995b; Coe et al., 1995). The immediately overlying flow was mainly overprinted by one or both of the two unusually thick post-gap flows, apparently having protected the critical flow from a similar fate, but it also displayed more subdued directional variation in the lower third that could not be fit with the same conductive cooling model.

Because the implied rate of field change was so astonishingly high, even higher than at the first gap where the critical flow is a little thicker, alternatives to the rapid-field-change hypothesis were explored (Coe et al., 1995). The most plausible was judged to be reheating during emplacement of the overlying flow or flows, causing a chemical remanence that for some reason was concentrated systematically toward a level in the lower half of the flow, because in this case the intermediate directions lay close to the great circle connecting the pre-gap and post-gap directions. Purely thermal overprinting could not explain the observations because its effect would be greatest at the top and decrease monotonically with depth in the flow. Moreover, conductive cooling models showed that baking by the overlying flows could not reach the high temperatures needed to thermally unblock enough of the remanence. But chemical alteration commonly produces remanence with unblocking temperatures much higher than the temperature at which it occurs. Thus chemical remanence with post-gap direction overlapping original thermoremanence with pre-gap direction could, in the right proportions, produce the intermediate high-temperature directions observed after thermal demagnetization to 500 °C. For this explanation to work, however, the interior part of the flow that has the most deviant directions would have to be the most susceptible to such chemical alteration, more so than immediately higher parts even though these would have been reheated to higher temperatures during baking. Much effort was expended searching for variation of material properties as a function of vertical position in the flow that might have predisposed it to such magnetochemical alteration. These included examination of polished thin sections, determination of thermomagnetic heating and cooling curves, and measurement of hysteresis parameters indicative of magnetic grain size (Coe et al., 1995), but no such predisposition was found.

Another way to test the rapid-field-change hypothesis is to examine how the same critical parts of the transition zone are recorded at other localities. If the directional gaps were due to greater than usual time elapsed between emplacement of successive flows rather than to rapid field change, then elsewhere in the Steens volcanic field there might be additional flows with directions filling the gap. The first attempt at this strategy involved extending sampling higher across the level of the second directional gap in the Steens B section. This is only 2 km from the Steens A section where the second directional gap was originally discovered

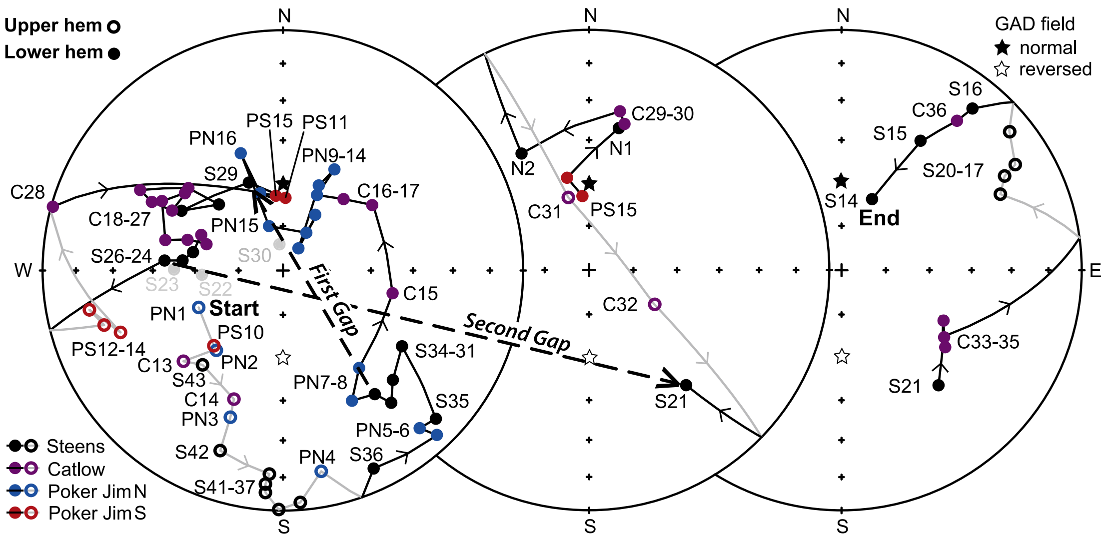

Fig. 2. The first and second directional gaps of the original record in Fig. 1 (dashed arrows) superimposed on the new composite path of the Steens reversal transition. The composite record (Jarboe et al., 2011) incorporated directions from three additional basaltic sections (label prefixes C = Catlow Peak, PN = Poker Jim North, PS = Poker Jim South) of the Steens volcanic field spliced into the earlier record of Mankinen et al. (1985) and Camps et al. (1999) from two sections at Steens Mountain (label prefixes S and N). The record starts (ends) on the left (right) panel. (The equally long second gap after including the two directions of Camps et al., 1999 would be from N2 to S21.) Each circle on the equal-area diagrams is a directional group comprising the mean direction of 5 to 121 samples from 1 to 14 sequential flows that have nearly identical directions; solid (hollow) circles indicate downward (upward) inclinations. Almost all reversed and normal directions from flows erupted before and after the transition are omitted for clarity. Also omitted are the 95% confidence limits for the directional groups, which range from 1.2 to 14.3°, two-thirds of them less than 5°. Steens directional groups S22, S23 and S30 (light gray) have been removed from the transition path because, as explained in the text, stepwise demagnetization did not isolate their characteristic remanences and we judge their primary directions to be those of their respective underlying flows. (Adapted from Fig. 15 of Jarboe et al., 2011.)

(Mankinen et al., 1985) and studied in detail nearby (Coe et al., 1995). Two new transitional directions were found at Steens B, one carried by one flow and the other carried by two flows (Camps et al., 1999). The simplest interpretation of these new directions weighed against the hypothesis of rapid field change, but, because an equally large gap still remained in the composite record with A and B results spliced together, the hypothesis could not be ruled out. The recent composite record of Jarboe et al. (2011), however, splices ten new directions into the gap in the Steens A path that were recorded by 17 flows from two much more distant sections, Poker Jim Ridge 80 km to the west of Steens Mountain and Catlow Peak 70 km to the south-southeast (Fig. 2). The simple ∼90° gap, which jumped from a NW-down to a SW-down direction, is replaced in the composite record by a sequence of directions comprising a complex path that is about five times as long as before and includes two forays onto the upper hemisphere. Thus the rapid-field-change hypothesis is no longer a viable explanation for the second directional gap exhibited in the original benchmark record of Mankinen et al. (1985). The best explanation is that some kind of rock-magnetic artifact produced the unusual signature of deviating directions of high-temperature remanence observed by Coe et al. (1995) in the Steens A flow at the gap, and that the field at the time this flow cooled was the same as the pre-gap direction recorded in the underlying flow. The proximity of the streaked high-temperature directions to the great circle connecting the pre- and post-gap directions shows that the cause is very likely chemical changes produced by heating from the overlying flows or flows, although the mechanism explaining the predisposition of the lower half of the flow to such remagnetization is still not known.

Nonetheless, the greater detail of the composite record (Fig. 2) does not preclude the rapid-field-change hypothesis for the first directional gap. Coe and Prévot (1989) noted that the streaked directions of high-temperature remanence that they found in the critical flow B51 deviated significantly from the great circle connecting the well-defined directions of the pre- and post-gap flows, not consistent with partial overprinting by chemical remanence acquired during heating by the overlying. Moreover, Fig. 3 shows that the twenty-two new flow directions in this part of the com-

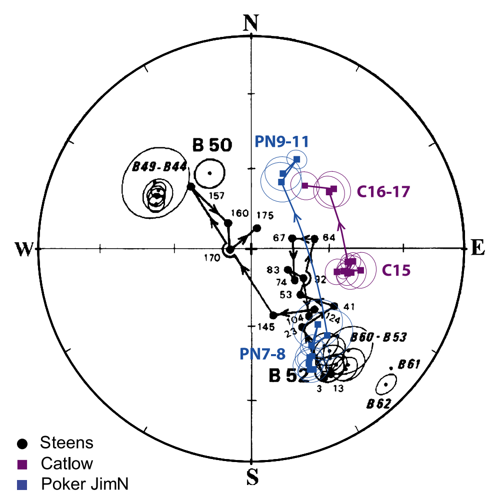

Fig. 3. Comparison between sections of records of the Steens Mountain reversal at the first directional gap. Steens Mountain section flows B44-B62, including the anomalously streaked directions of flow B51 from Fig. 1c are shown as filled circles with labels indicating height in centimeters above the base. Filled squares show flows at the equivalent levels at Poker Jim North (directional groups PN7-11) and Catlow Peak (directional groups C15-17). The important observation is that the directional trends of the Poker Jim and Catlow flows parallel those from the samples in the lower two-thirds of flow B51 and leave large gaps that would still permit the rapid-field-change hypothesis.

posite record trend parallel to the streaked directions that were observed in the samples spanning the interior portion of flow B51. These new flows define only three clumps of directions with large gaps between them, still leaving room for the rapid-field-change hypothesis.

Bearing in mind the considerable uncertainties in transitional field directions, which in this case were accompanied by very weak intensities perhaps as low as ten percent of the present field, the similarities between the enigmatic streaked directions of the Steens B flow at the first directional gap and the directions of the new flows of the composite record shown in Fig. 3 could be regarded either as a coincidence or as supporting the rapid-field-change hypothesis. This ambiguity demanded further study, and because no samples remained we mounted an expedition to collect again from this critical flow. We repeated the original demagnetization experiments and performed many others. As a result we are now able to show convincingly that the puzzling streaked directions in this flow are not primary recordings of a rapidly changing field, but rather are also a rock-magnetic artifact, although necessarily different from whatever produced the streaked directions in the Steens A flow in the second directional gap because of the different magnetic properties of the two flows at each gap.

This conclusion, though perhaps mundane, is important to set the record straight. Besides its influence in the professional and lay scientific literature, the Steens rapid-field-hypothesis was included in a widely-aired TV documentary (Copp, 2003a, 2003b), was applied to the Laschamp event in a science-fiction novel (Sawyer, 2003), and was misinterpreted by creationists in their attempts to reconcile the geological and biblical time scales (*e.g.*, Humphreys, 1990). Moreover, because subaerial lava flows are generally regarded as the gold standard of paleomagnetic recorders, understanding how the remanence of this unusual flow formed provides valuable insight into basaltic rock magnetism that will help improve interpretation of other data.

2. Sample collection

The flow numbers in the Steens B section increase downward from the top. Where sampled at the first directional gap, the critical flow B51 is 1.9 m thick and is overlain by 2.3 m thick flow B50 that is magnetized northwest and downward. It is underlain by flow B52 and eight successively lower flows with southwest and downward directions that are not significantly different from each other (Fig. 1c). B51 is a simple, well-exposed flow with a sharp base, a massive fine-grained interior almost devoid of vesicles, and a vesicular, well-exposed top. It is generally fresh except for the top 20 cm, which is reddish in places and less hard than the rest. The flow shows no signs of having grown by inflation, so it would be expected to have cooled normally through its magnetic blocking temperature range according to a simple conductive cooling model, such as the one applied to the flow at the second gap by Camps et al. (1995b) and Coe et al. (1995) but with cooling times about twice as long to account for the greater thickness of flow B51.

In resampling this part of Steens B we drilled paleomagnetic core samples in two nearly vertical sections at the location of the original Coe and Prévot (1989) study (N42°37.667′, W118°34.014′; see Figure S-4 location map and images in the Supplementary Material). The drilling angle was approximately horizontal and the cores provided one to three standard 2.5 cm samples each. The first section follows the same line as the earlier study, with twenty-one cores spanning all but the top 0.2 m of the critical flow B51 and four samples continuing 0.5 m down into the underlying flow B52 (Supplementary Table S-1). The second section is 3 m to the south, with nineteen samples spanning the thickness of flow B51 there plus five samples extending 1.1 m down into B52 and five samples extending up into the overlying flow B50. The orientation error is ±2° or less, with the measured magnetic azimuths of all cores corrected using the observed azimuth of the sun. In this paper we concentrate on the first section, so as to compare directly with the earlier study, but the magnetic behavior in both sections is similar.

3. Paleomagnetic directions

3.1. The bounding flows

Relatively few cores were taken from the flows immediately above and below the critical flow because their behavior was straightforward in the study of Mankinen et al. (1985). After removal of a low-stability component, thermal and alternating-field (AF) demagnetization of most samples yielded directions of characteristic remanence (ChRM) that are consistent with the previous study (Table S-1, flows B50 and B52). They exhibit the high unblocking temperatures and median destructive fields typical of high-temperature oxidized basalt, with half their remanence concentrated above 500 °C or 50 mT.

3.2. The critical flow (B51)

3.2.1. Alternating-field demagnetization

To save material for other experiments, we used half a standard 2.5 cm sample in our automated system, which demagnetizes samples in a Sapphire Instruments solenoid and measures them in a 2G superconducting magnetometer equipped with a sample handler employing twelve symmetric orientations per measurement (Morris et al., 2009). Typical demagnetizations comprised eighteen AF steps up to 180 mT. The directions of natural remanence for all samples before demagnetization are steeply downward, suggesting a large normal polarity overprint. The mean NRM declination omitting only samples from the highest cores and from the two lowest cores in the vertical profile is zero, consistent with the normal polarity axial dipole direction, but the mean inclination is 15° steeper. The median destructive AF field is unusually low, ranging from 2–10 mT for all but the uppermost and lowermost core. During progressive AF demagnetization the sample directions generally move a little toward the direction of the underlying flow and spread farther apart. Individual ChRMs determined from vector component diagrams are reasonably well defined but differ by up to 90°. Even ignoring the four samples nearest the bounding flows, which deviate the most from the rest, the angular spread is 50° (Table S-1). These characteristics are typical in paleomagnetic studies where varying amounts of two or more overlapping components cannot be separated by AF demagnetization.

3.2.2. Thermal demagnetization

If these overlapping components were thermal or viscous overprints superimposed on primary TRM, then the usual expectation would be that thermal demagnetization could separate them successfully. We thermally demagnetized batches of ten to twelve samples in a custom designed and built oven in a magnetically shielded room. The ambient magnetic field in the region where the samples cool is less than 0.02 μT. The spacing between samples ensured that the field produced by the remanence of any sample on its neighbors did not exceed 0.03 μT, and usually was far less. However, when we determined their remanent magnetization after each heating-cooling step in the 2G superconducting magnetometer, all samples except those from the margins of flow B51 failed to display demagnetization trajectories that trend convincingly toward the origin of vector diagrams. As illustrated in Fig. 4, the direction during progressive thermal demagnetization drifts halfway toward that of the underlying flow until it becomes unstable above 500 °C. This behavior was not unexpected because it resembles closely the anomalous behavior displayed in the earlier study for a sample from virtually the same position in the flow (*cf.* Fig. 3 in Coe and Prévot, 1989).

Lacking stable endpoints, Coe and Prévot (1989) decided that the best way to compare the directions of stable magnetization as a function of position in flow B51 is to plot the 500 °C step, the temperature just below which the direction starts jumping around erratically at the tail end of demagnetization. The directions obtained in the present study for the 500 °C step are given in Table S-1. These are plotted in Fig. 5 as a function of height above base, averaged over a few successive samples for clarity, and compared with the earlier study. The general agreement is

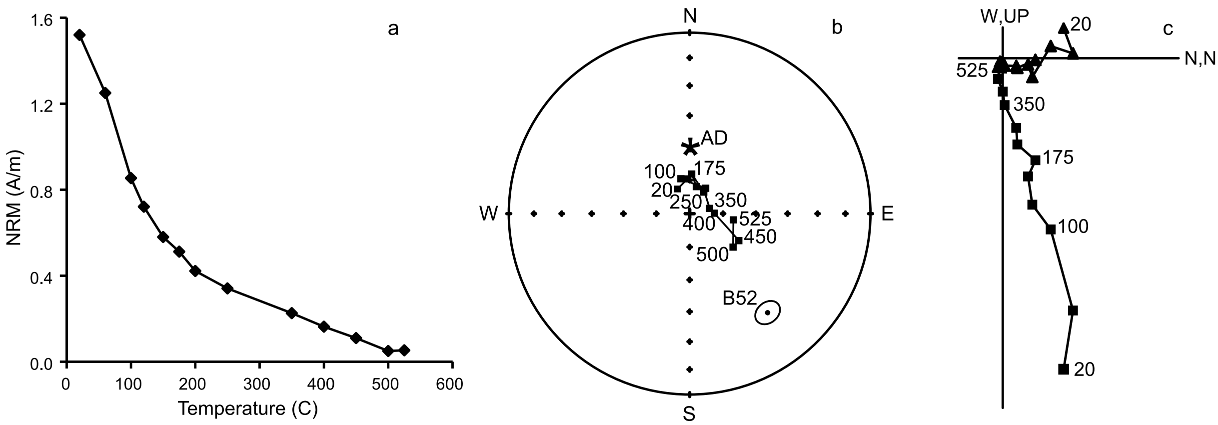

Fig. 4. Conventional thermal demagnetization of natural remanent magnetization of a sample from flow B51 sample located 42 cm the base. (a) Decay of intensity with temperature. (b) Change in direction with temperature. Axial dipole (AD) and underlying flow (B52) directions are shown for reference. (c) Zijderveld diagram showing change with temperature of components in the horizontal (triangles) and N-S vertical (squares) planes.

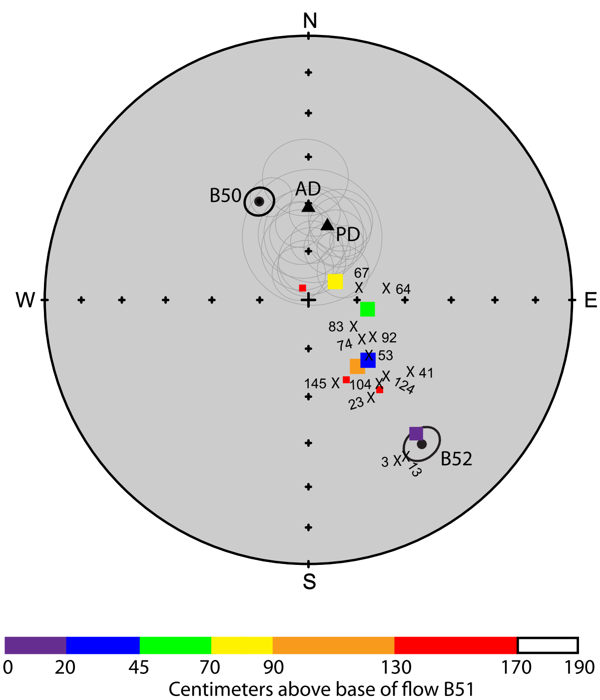

Fig. 5. Directions of magnetization of flow B51 samples after treatment by conventional thermal demagnetization. Each large square is the average direction, after demagnetization in this study to 500 °C, for successive samples contained within the height-above-base range indicated on the bar below. See Table S-1 for the individual direction of each sample. Smaller squares are individual sample directions for the uppermost 130–170 cm range, which are variably affected by baking and too scattered to justify averaging. No samples were collected above 170 cm. Small black crosses are 500 °C directions for samples from the previous study of Coe and Prévot (1989), with small numbers indicating height in centimeters above the base of flow B51. Note how in both the 1989 and this study the directions of samples progressively higher above the base move away from the underlying flow B52 direction and then back again toward it. The 60–200 °C least-square-fit directions of each sample indicated by thin gray 95-percent confidence circles are consistent with normal-field overprinting, showing similarities to the present-day (PD), axial dipole (AD), and overlying flow B50 directions.

good. Sample directions closest to the base of the flow plot next to the underlying flow B52 direction, and then with increasing height their directions move further away until a level somewhat below the middle. Above this point the samples exhibit the behavior that formed the basis for the rapid-field-change hypothesis, their average direction trending back the other way toward that of the underlying flow. This sort of variation cannot be explained by thermoviscous overprinting due to simple baking by the overlying flow because the higher baking temperature would produce more rather than less overprint. It is the sort of variation that would occur if the field changed direction appreciably as the flow cooled, but as before the rate implied would have to be extremely fast, at least several degrees per day.

3.2.3. *Continuous thermal demagnetization*

Coe and Prévot (1989) briefly entertained an alternative hypothesis that normal-polarity viscous remanent magnetization (VRM) had not been completely removed, and that the streaked-out directions of 500 °C remanence were the result of residual VRM mixed with primary TRM acquired in a field with the same direction as that recorded by the underlying flow. They dismissed this possibility because the sharp drop in intensity during demagnetization up to 200 °C followed by much slower subsequent decay up to 500 °C suggested that thermal demagnetization had completely removed VRM. Indeed, we observe similar demagnetization behavior in our new samples (Fig. 4). Nonetheless, to check if alteration during conventional thermal demagnetization were playing an unexpected role, we decided to try continuous thermal demagnetization (*e.g.*, Creer, 1967) in the Triaxe vibrating sample magnetometer at the Institute of Physics of the Globe in Paris, which has the advantage of much shorter exposure of samples to high temperatures.

The Triaxe vibrating sample magnetometer was designed to enable rapid, automated paleointensity determinations (Le Goff and Gallet, 2004). It can measure all three axes of the moment of a cylindrical sample with a sensitivity of better than 10^{-8} Am^2 while heating it continuously in a non-inductively wound furnace within a magnetic shield. The small sample size (~0.75 by 1 cm in diameter and length), while reducing the accuracy of azimuthal orientation somewhat to around ±5°, greatly facilitates rapid heating, so an entire thermal demagnetization took only 12.5 min. This ability proved critical, as illustrated in Fig. 6a. The direction during demagnetization in the Triaxe moves beside the path traced out during stepwise thermal demagnetization of its sister sample (Fig. 4), continuing all the way to that of the underlying flow. Of the fourteen samples from flow B51 that we demagnetized successfully with the Triaxe, thirteen displayed similar behavior. They all reached endpoint directions near the mean direction of the underlying flow (Table S-1), and their mean direction is indistinguishable from it at 95% confidence (Fig. 6b). The exception was sample 25A, the uppermost of the fourteen, just 32 cm below the contact with the overlying flow. Its direction moved only 12° during continuous thermal demagnetization, along a path away from the overlying and toward the underlying flow direction. Clearly it was heavily overprinted during baking when flow B50 was emplaced above it.

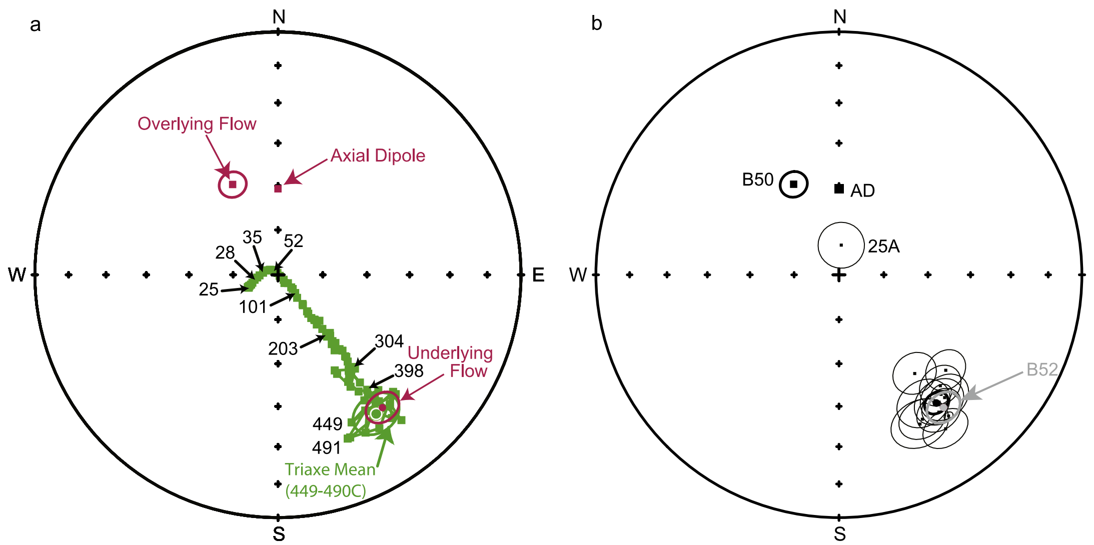

Fig. 6. (a) Continuous thermal demagnetization in the Triaxe vibrating sample magnetometer (Le Goff and Gallet, 2004) of sample 10A, 42 cm above the base of flow B51. Black numbers indicate temperatures along the demagnetization path. A stable endpoint is reached by 449 °C, and the mean direction above this temperature is indistinguishable within error from the direction of the underlying flow B52. Directions of the overlying flow B50 and the axial dipole (AD) are shown for reference. (b) Stable-endpoint directions and 95% confidence circles of the 14 samples of flow B51 demagnetized continuously in the Triaxe. Except for sample 25A that is closest to and therefore most baked by the overlying flow, all cluster around the direction of the underlying flow (gray circle) and yield a mean (black circle) indistinguishable from it.

These results constitute unambiguous evidence in favor of the alternative hypothesis. Demagnetization in the Triaxe isolated a high-temperature component in the NRM that stepwise thermal demagnetization failed to separate. Both types of demagnetization demonstrate that the samples contain a normal-polarity low-temperature remanence, which is consistent with overprinting by a combination of Brunhes-age VRM and thermoviscous and chemical remanent magnetization from heating by the overlying flow, but only the rapid continuous demagnetization performed by the Triaxe was able to remove the overprint cleanly and reveal the primary direction at high-temperature. It is the same within error as the direction of the underlying flow, B52, and for that matter essentially the same as the directions of the eight flows below that (B53–B60). The failure of conventional stepwise thermal demagnetization to isolate the primary direction can be explained by the much longer time spent at elevated temperature in that method: each of the many heating-cooling steps took 45–60 min, as opposed to 12–13 min for the entire continuous demagnetization process in the Triaxe. Alteration of magnetic minerals carrying the overprint direction must have occurred at relatively low-temperature during conventional thermal demagnetization, raising its unblocking temperature before it was entirely erased so that it could never be separated from the primary remanence. The question remains, however, what are the material properties of flow B51 that are responsible for this deceptive behavior, so we now turn to an investigation of its rock-magnetic behavior.

4. Rock magnetic properties

Standard paleomagnetic techniques could not recover the primary direction of magnetization that we are now sure most samples of flow B51 still carried. Alternating field and stepwise thermal demagnetization succeeded on only two samples, which lay within 20 cm of the base, and failed throughout the upper ninety percent of the flow. Fortunately, rapid continuous thermal demagnetization in the Triaxe did succeed on samples, with the exception of one strongly baked sample only 32 cm below the top. However, flow bases are often covered, and magnetic mineral alteration might occur too quickly during heating of samples from some other flows for continuous thermal demagnetization to work. Thus it is important to try to understand the rock magnetic properties of flow B51 that are responsible for its unusual paleomagnetic behavior so as to avoid misinterpreting thermally and AF-cleaned remanence as primary in similar cases.

4.1. Thermomagnetic measurements

We measured both the variation of initial susceptibility (k) and strong-field magnetization (Ms) with temperature (T) in air with an Agico MFK1 Kappabridge and a Variable Field Translation Balance (VFTB, Krása et al., 2005), respectively. Although the Ms–T curves are more subdued than the k–T curves because of the higher field employed (0.7 T), they revealed Curie temperatures that agree quite well with each other, especially when using the inflection point for the latter (Petrovský and Kapička, 2006; Fabian et al., 2006) and the two-tangent intersection for the former (Grommé et al., 1969). Irreversibility in thermomagnetic measurements signals magnetic mineral alteration, and progressively increasing heating-cooling cycles can show at what temperature it becomes apparent. The Kappabridge k–T cycles proved more sensitive for this purpose, whereas the VFTB Ms–T curves are more straightforward to interpret because, unlike initial susceptibility, saturation magnetization is an intrinsic property not dependent on grain-size, crystal imperfections, and so on.

Thermal cycles of magnetic susceptibility (k–T), performed in air on a sample from a little below the center of flow B51, show the emergence of irreversibility at 307 °C that becomes more and more pronounced at higher temperatures (Fig. 7a). These k–T curves also indicate that the pristine sample possessed at least two magnetic phases, one with a Curie temperature around 100 °C and another with a higher Curie temperature, probably around 450–475 °C. The original Curie point of this second phase in the unheated specimen is uncertain, however, because its temperature increases with each successive cycle above 458 °C as the magnetic mineralogy alters, finally reaching a maximum value just above 500 °C. Moreover, a third, even higher-temperature phase is apparent in the three highest temperature cycles, with a Curie temperature of 570 °C in the last cycle. But did this highest Curie temperature phase exist in the pristine specimen, or did heating in the Kappabridge produce it?

In an attempt to answer this question we tried running the k–T cycles in an argon atmosphere, but this never lessened the

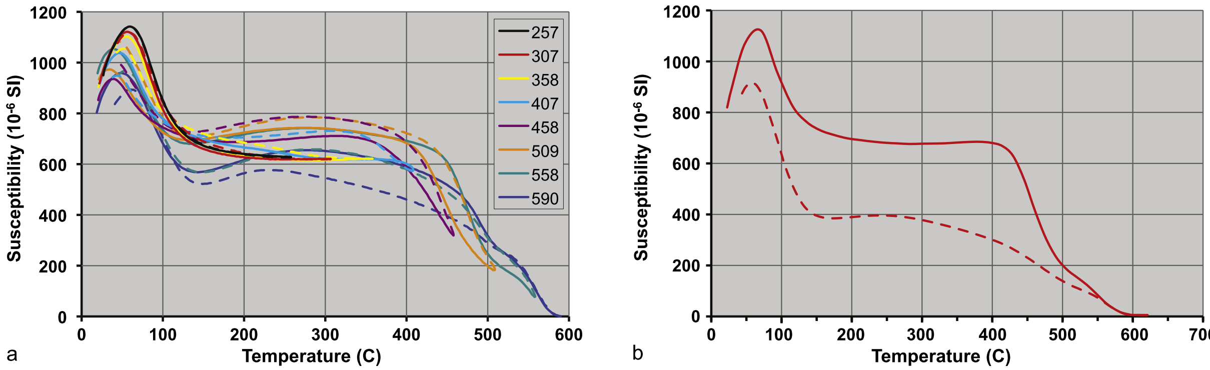

Fig. 7. Thermomagnetic cycles of susceptibility measured in the Kappabridge in air. (a) Cycles to progressively higher temperatures for sample 19, 86 cm above the base of flow B51, with a standard heating rate of 12 °C/min. Irreversibility of the heating (solid lines) and cooling (dashed lines) curves indicate chemical changes occurring around 300 °C and above. Note the three Curie temperatures displayed: a stable one at about 100 °C, an unstable one first detectable at ∼450 °C that progressively increases to ∼500 °C, and a third one at ∼560 °C visible in the last cycle. (b) A single cycle at a very fast heating rate (∼45C/min) for a piece of the same sample as in (a). Note that the same three Curie temperatures are displayed, suggesting that they all existed in the sample before heating.

irreversibility and sometimes even made it worse. So instead we subjected a fresh specimen from the same core to a very rapid k–T cycle to 621 °C in air, the idea being to minimize alteration during heating (Fig. 7b). The heating rate was ∼45°/min, comparable to the rate during continuous thermal demagnetization in the Triaxe and about four times the rate for the multiple cycles of the previous figure. Even though this sample spent much less time at high temperature than the previous sample, its heating curve still exhibits the same two phases with Curie temperatures around 100 °C and 475 °C we inferred before and also the third phase with Curie temperature between 550 and 580 °C. Thus it is likely that the three phases were present in this sample before laboratory heating. The same appears to be true for all the samples except for the two closest to the base and to the top of the flow, as shown by Ms–T cycles performed in the VFTB on eleven samples spanning flow B51 (Supplemental Figure S-1). They again reveal varying amounts of phases with Curie temperatures around 100–150 °C, 400–500 °C, 500–580 °C and show distinct irreversibility beginning between 300 and 400 °C. Similar two- and sometimes three-Curie temperature assemblages have been reported in other studies of basalt flows (*e.g.*, Camps et al., 2011).

4.2. Microscopy

Observations of polished sections under reflected light in air with a Leitz Ortholux Plan microscope reveal a preponderance of blocky, strongly reflecting grains, 20–50 microns in size and mainly euhedral, with a tail in the distribution extending down to 5–10 microns and lower, and a sprinkling of bright skinny laths 2–7 microns wide by tens of microns long (Figure S-2a). In oil immersion the blocky grains display the light tan color typical of titanomagnetite (Figure S-2b). They attract magnetic colloid, conferring a reddish brown color that shows that they are strongly magnetic, but many of them do so unevenly, suggesting patches of alteration to a less magnetic phase (Figure S-2c). Etching the polished surface with dilute hydrofluoric acid for 45–60 s reveals fine curved cracks, long known to occur by shrinking of the host titanomagnetite lattice during oxidation to cation-deficient titanomaghemite (Larson and Strangway, 1969). Most of the laths do not attract magnetic colloid and are likely nonmagnetic ilmenite.

These observations are remarkably similar to those described by Petersen et al. (1979) in some sea-floor basalt samples, and especially to those presented and discussed in detail by Krása et al. (2005) for the Olby basalt flow in France (compare our Figure S-2a and b with Krása et al.'s Figs. 8 and 9). Those authors argue convincingly that the dominant alteration is localized maghemitization within the titanomagnetite grains by varying degrees of low-

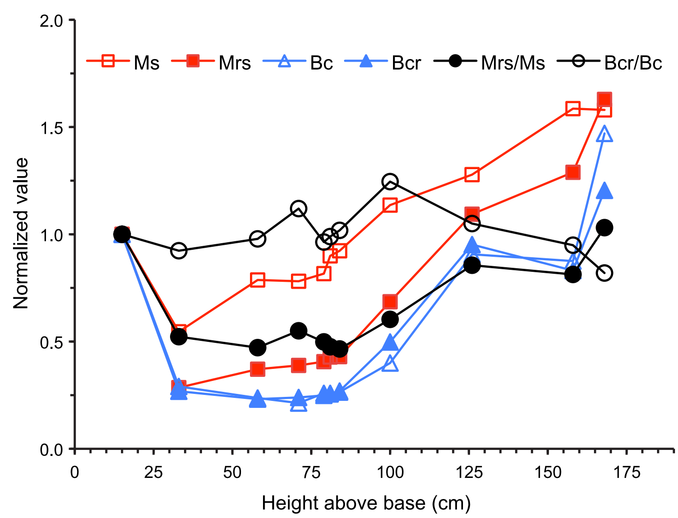

Fig. 8. The variation in magnetic hysteresis parameters of flow B51 with height above the base. Ms = saturation magnetization; Mrs = saturation remanence; Bc = coercivity; Bcr = remanent coercivity. All measurements made in the variable frequency translation balance.

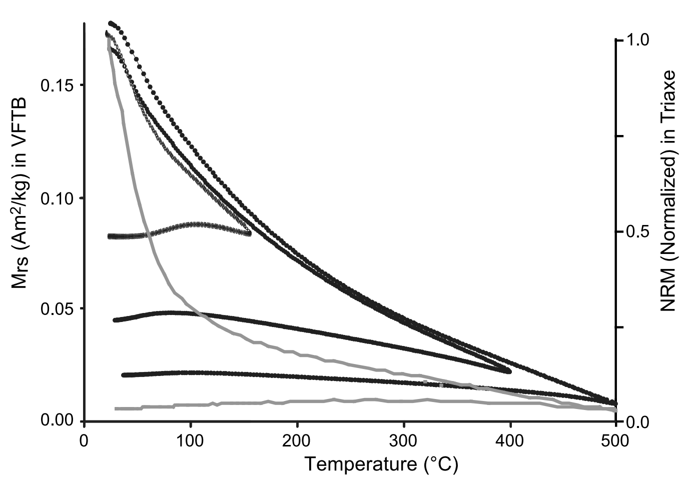

Fig. 9. Continuous thermal demagnetization showing negative interaction between high- and low-unblocking-temperature phases in samples from flow B51. Negative interactions are evident by the diminishing magnitude of slope and eventually of magnetization itself in the cooling curves. Black lines: heating-cooling cycles to progressively higher temperatures of saturation remanence (Mrs) for sample 16B in the variable frequency translation balance. Gray lines: a heating-cooling cycle to 500 °C of natural remanence (NRM) for sample 18B in the Triaxe vibrating sample magnetometer.

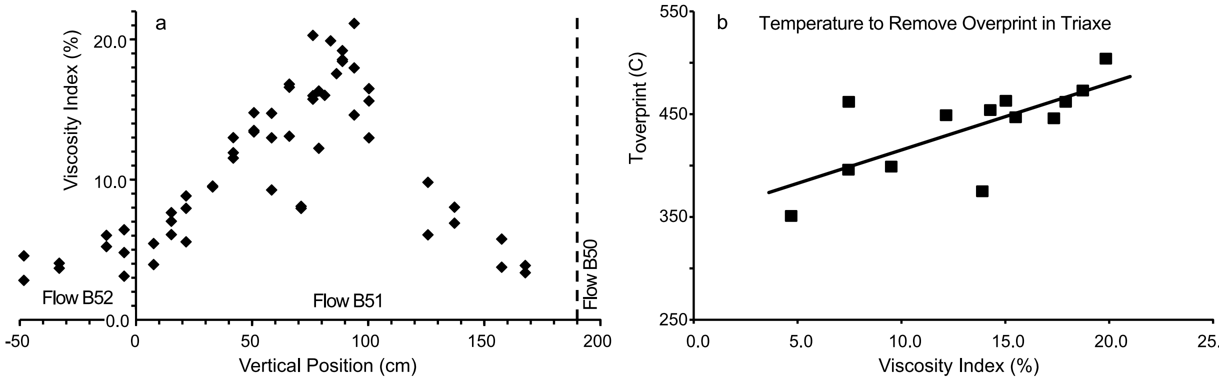

Fig. 10. Importance of viscous remanent magnetization in flow B51. (a) The viscosity index, determined from ∼ two-week storage experiments, varies systematically with height above base in flow B51, reaching an unusually high value around 20% just below the center. (b) The minimum temperature at which the normal-polarity overprint is completely removed during continuous thermal demagnetization in the Triaxe. Note that it is generally higher for samples with higher viscosity index.

temperature oxidation to titanomaghemite. By 'low-temperature' they simply meant low enough that oxy-exsolution of grains to form alternating lamellae of magnetite and ilmenite is suppressed, but still occurring during cooling of the flow in their interpretation. In addition, as reported by Heller and Petersen (1982) in the Olby flow and Camps et al. (2011) in some Icelandic basalts, we have also observed a few instances of grains in flow B51 with lamellae indicating minor oxy-exsolution coexisting with both pristine and modestly low-temperature oxidized titanomagnetite grains.

4.3. Hysteresis

We measured magnetic hysteresis of small chips (5–40 mg) and cylindrical sub-samples (6 mm diameter, 300–500 mg) using an alternating gradient magnetometer (AGM, Princeton Measurements Corporation 2900) and a VFTB, respectively. Results of the two instruments agreed well, though those on the VFTB are surely a better average because of the ten times larger sample size. The hysteresis loops for flow B51 are upright, saturating by 0.5 T, except for samples nearest the top that are not fully saturated until 0.75 T. Loops of samples from the interior are rather low coercivity (∼5 mT) and very slightly wasp-waisted. Measurements using the VFTB, displayed in Table S-2 and Fig. 8, reveal systematic changes in hysteresis parameters as a function of height in the flow. Magnetic coercivity Bc and coercivity of remanence Bcr both decrease dramatically inward from the margins. Saturation magnetization Ms and remanence Mrs also decrease inward, the latter more steeply than the former. All four are somewhat greater near the top than near the bottom, and the smallest values are found in the lower interior part of the flow. The effective-magnetic-grain-size proxy Mrs/Ms ratio is about 50% smaller in the lower interior than at the margins, but the other grain-size proxy Bcr/Bc remains more or less constant. In general, the variation in hysteresis and thermomagnetic properties suggests that the profile of hysteresis parameters reflects mainly cooling rate at the time of emplacement, but also greater access at the margins to oxygen and increasing degree of reheating upward in flow B51 by the emplacement of B50 on top of it.

4.4. Interactions

The thermoremanence of almost all samples of flow B51 during partial demagnetization in the Triaxe displayed modest negative magnetic interactions as they cooled in zero field. Fig. 9 shows the most pronounced example, from sample 16B a little below the middle of the flow, but the only exceptions were the lowest and highest samples tested, 8 and 33 cm above the base and below the top, respectively. If there were no such interaction the cooling curve would have to increase monotonically because the spontaneous magnetization does so. Instead, the cooling curves for the more interior samples, starting from a temperature at which the magnetization was only 2–12% of the NRM, leveled off around 250–350 °C and then decreased. In some others the decrease was not evident until cooling below 120–150 °C. The interaction component is approximately antiparallel to the residual high-temperature remanence, and in no cases did the remanence reverse polarity during cooling.

The purpose of the Triaxe experiments was to isolate the highest-temperature remanence quickly, not to study interactions. Thus, after demagnetization to high temperature, there was only a small amount of magnetization remaining in some samples that could produce detectable interaction remanence during cooling. To make sure the observation of magnetic interaction was robust, we also performed a few continuous thermal demagnetization experiments in the VFTB on saturation remanence of a sample slightly below the middle of flow B51 (Fig. 9). After saturation in the VFTB in 840 mT, the field was reduced as close to zero as feasible (∼0.02 mT) and the sample was heated to 156 °C and cooled to ambient temperature. This process was repeated two more times with heating to 399 and 498 °C. In all three cases the remanence on cooling reaches a maximum in the vicinity of 100 °C and then decreases. As expected, the maximum is most pronounced for the lowest-temperature cycle, when most of the remanence remains to couple negatively to that already demagnetized. Of course, the magnetic interactions surely must have produced opposing partial thermoremanence at temperatures above the maximum, too, anywhere along the cooling curve where the magnetization rises less steeply than the *Ms*–*T* curve.

4.5. Viscosity test

A variant of the storage test of Thellier and Thellier (1944) showed that the interior of flow B51 is unusually viscous. All the samples were stored in nearly zero field in the shielded room in Santa Cruz for many weeks. Their vector remanence **NRM1** was measured and then they were stored in today's field without moving for 11–14 days and remeasured (**NRM2**). The values of viscosity index, $V = 100(|\mathbf{NRM2} - \mathbf{NRM1}|)/|\mathbf{NRM1}|$, are listed in Table S-1 for all the samples and plotted versus height above base for Section 1 in Fig. 10a. It increases progressively from 3–5% nearest the margins to a maximum as high as 22% for samples in the 10 cm interval just below the middle. Nonetheless, even knowing about the high viscosity, the break in slope of the thermal demagnetization intensity curve obtained before by Coe and Prévot (1989), and again by us in this study (Fig. 4), can easily give the false impression that almost all VRM was removed by 175–200 °C and thus entirely erased by 450–500 °C.

5. Discussion and interpretation

The most obvious factors that could affect the variation in mineral-magnetic properties along a vertical profile in flow B51 are (*i*) primary cooling rate (fastest near the margins, especially the top), (*ii*) access to oxygen (easier at the top and sometimes also at the bottom), and (*iii*) degree of reheating (strictly a top-down effect). With regard to (*i*), quenching of small-size magnetic grains at the margins that continue to grow inside is consistent with the general variation of hysteresis parameters in B51 (Fig. 8). For (*ii*), indications from thermomagnetic curves of nearly pure magnetite near the top and bottom and a nearly unoxidized titanomagnetite phase in the interior is consistent with enhanced access to oxygen from the outside. Note, however, that de Groot et al. (2014) have documented the opposite trend in a much thicker (6 m) flow in Hawaii, where degree of oxidation appears to have been controlled instead by cooling rate. The high-Curie-temperature phases that dominate at the margins were likely formed by oxy-exsolution at high-temperature, implying further reduction in effective magnetic grain size, consistent with the hysteresis results. As for (*iii*), later reheating by the overlying flow and further oxidation may explain why all the hysteresis parameters except Bcr/Bc are greater near the top than near the bottom. Much more challenging than drawing these simple correlations, however, is understanding the behavior of remanence and the failure of conventional demagnetization techniques to isolate the primary direction of magnetization of samples from the interior of the flow, to which we now turn.

Considerable attention has been devoted over the years to basalts that exhibit negative interactions between the partial TRMs of two magnetic phases with different Curie temperatures (*e.g.*, Nagata and Ozima, 1955; Havard and Lewis, 1965; Creer and Petersen, 1969; Creer et al., 1970; Heller and Petersen, 1982; Krása et al., 2005; Draeger et al., 2006). The relevance of these studies for this paper is not the negative interactions themselves, which are relatively weak in Steens flow B51 and not responsible for the failure of conventional thermal demagnetization to isolate the primary TRM direction. Rather, their relevance is that many, perhaps all, concern magnetically viscous basalts that contain both low- and higher-Curie-temperature phases attributable to titanomagnetite and titanomaghemite (including its even higher-Curie-point inversion products when present), respectively. In their comprehensive study of the Olby flow, Krása et al. (2005) made a strong case based on both observation and modeling that the self-reversing behavior arises from magnetostatic interaction within titanomagnetite grains and patches of titanomaghemite produced by localized low-temperature oxidation of the host. Most important for our purposes, they demonstrated that it is the alteration product that carries the primary direction of the earth's field because it formed and became magnetized during cooling at temperatures above the Curie point of its host.

Hoffman (1984) reported briefly on variable remanent directions remaining after demagnetization in samples distributed within a basalt flow in the Oligocene Liverpool volcanics of eastern Australia. On the face of it, this flow bears even more resemblance to Steens B51 because it occurs in a polarity transition zone, it exhibits an unusually low Curie temperature of ∼100 °C, and it contains nearly unaltered large grains of titanomagnetite assumed to have undergone some spotty low-temperature oxidation to titanomaghemite during primary cooling and, in some samples, also later at ambient temperature. The major differences from our study are that AF demagnetization was able to isolate the inferred primary direction of magnetization for most samples, which was the same as the unusual shallow reversed direction found in the next higher flow, and that detailed *conventional* thermal demagnetization was successful for the most heavily overprinted samples that AF could not clean up. Hoffman concluded that (*i*) the stable primary remanence resides in titanomaghemite and in occasional high-temperature-oxidized grains formed as the flow cooled and (*ii*) the secondary overprint is CRM arising from later low-temperature oxidation at ambient temperature.

In Steens flow B51 the failure of both conventional AF and thermal demagnetization to obtain consistent stable-endpoint directions was not the main reason for the rapid-field-change hypothesis. Most convincing for us (Coe and Prévot, 1989) was the way that the remanence remaining after the 500 °C demagnetization step changed direction as a function of sample height in the flow. The variation resembles what would be expected if the field direction moved continuously as the flow acquired its TRM during cooling (Fig. 1c), and in the present study we found a similar pattern (Fig. 5). But rapid, continuous thermal demagnetization in the Triaxe of sister samples from the same core proves that this hypothesis is wrong. With this demagnetization technique they do reach stable endpoints that are listed in supplemental Table S-1 (see Figs. 6a and Figure S-3abc for examples), and their directions converge and cluster near the well-defined mean direction of the underlying flow (Fig. 6b). The temperature that the direction of each sample first reaches its stable cluster varies with sample height, ranging from around 375 °C to a little over 500 °C, and generally increases with viscosity coefficient (Fig. 10b). Considering the small size of samples used in the Triaxe and the considerable variability of viscosity index exhibited among some standard-size sister samples from the same core (Table S-1), the correlation is reasonably good and, we think, significant. It suggests that most of the persistent normal overprint, which only rapid continuous demagnetization could faithfully separate from the primary direction, was originally viscous—but likely affected by low-temperature oxidation, as explained at the end of this section.

There is more to the story, however, because conventional demagnetization techniques, both thermal and AF, are usually successful at removing VRM in basaltic rocks. This is certainly the case for the great majority of Steens basalt flows, which clean up to give tightly clustered sample directions and flow-means with small uncertainties (*e.g.*, Mankinen et al., 1985; Jarboe et al., 2008 and 2011). The success of rapid continuous thermal demagnetization over the standard stepwise technique, however, shows that the shorter time spent at temperature with the Triaxe was critical. Thus multidomain tails extending to high unblocking temperatures (*e.g.*, Dunlop and Özdemir, 2000) cannot explain the different results, because spending a shorter time in zero field would offer no advantage during demagnetization. What can explain the difference is alteration during laboratory heating that raises the unblocking temperature of a normal-polarity overprint while preserving its direction of magnetization. This overprint is likely a product of remanence acquired during the 780 kyr current normal polarity chron and remanence acquired during the much shorter baking time after emplacement of the overlying flow. The latter would be a combination of VRM and chemical remanent magnetization (CRM) formed at moderately elevated temperatures plus partial TRM formed during cooling. The inferred alteration during conventional thermal demagnetization, which is corroborated by the irreversibility and increases in Curie temperature exhibited by flow B51 samples in progressive thermomagnetic cycles (Figs. 7a and S-1), is probably incremental inversion of titanomaghemite plus some oxidation of titanomagnetite at higher temperatures (550 °C and above). Time and temperature trade off in both these thermally activated processes, with the happy result that the much faster continuous thermal demagnetization was able to outrun the alteration and erase the VRM before its unblocking temperatures were raised enough to comingle with those of the primary remanence.

Less clear is what magnetic grains carry the normal overprint that gets promoted to higher unblocking temperature during laboratory heating. We found that the samples more difficult to clean up with continuous thermal demagnetization are generally the ones with higher viscosity index (Fig. 10b). VRM is associated with low unblocking temperatures, and thus one might most readily associate it with the ∼100 °C Curie temperature phase that we tend to equate with the large titanomagnetite grains observed microscopically (Figure S-2). However, this temperature is too low for its remanence not to have been erased during stepwise thermal demagnetization long before it could oxidize and obscure the primary remanence. Perhaps the phase whose unblocking temperatures are raised during heating in the laboratory is the titanomaghemite in the already altered regions that are observed in the titanomagnetite host grains, but it could also be undetected submicroscopic magnetic grains of titanomaghemite or some unknown magnetic nanophase. These are open questions yet to be resolved.

6. Conclusions and further implications

The case for two episodes of extraordinarily rapid field change to explain suggestive streaking of directions within individual flows at prominent directional gaps in the Steens Mountain reversal record is now untenable. In particular, very rapid continuous thermal demagnetization accomplished in less than fifteen minutes in the Triaxe vibrating-sample magnetometer shows that the systematically streaked high-temperature directions exhibited by samples within flow B51 at the first directional gap are caused instead by systematic alteration occurring during the much longer time at elevated temperatures taken by conventional stepwise thermal demagnetization. In the Triaxe the flow B51 directions shown in Fig. 6a converge nicely to the stable direction of the underlying flow obtained by conventional AF and thermal cleaning. And even though the rock-magnetic mechanism for the streaked directions at the second directional gap is not yet known, the many new transitional directions at this point in the Steens reversal from two other sections (Fig. 3) show that the gap in the record at the original section must be explained instead by an unusually long temporal gap between superposed flows (Jarboe et al., 2011).

Most labs do not have instruments for performing continuous thermal demagnetization with three-component measurement of natural remanence, but our study of flow B51 reveals some easily measured rock-magnetic risk factors that may help avoid being misled. One is unusually high viscosity index, systematically higher in the interior than at the flow margins, which appears to have played a prominent role and can be determined by simple storage tests. It signals that a large low-temperature overprint compared to the primary remanence is probably harbored in the NRM. Another is presence of irreversibility in thermomagnetic curves of samples possessing two or more magnetic phases in which the Curie point of a low-temperature phase rises progressively with temperature. This can indicate progressive alteration of titanomaghemite or low-temperature oxidation of titanomagnetite, which could raise the blocking temperature while preserving the direction of a low-temperature overprint during thermal demagnetization. In addition, such samples are particularly prone to drilling overprints, so it is prudent to drill gently and use plenty of cooling water.

Regarding the question of episodes of unusually rapid field change, paleointensity studies of baked archeological materials by Gallet et al. (2013) and Genevey et al. (2013) suggest rates up to 0.3 and 0.5 nT/day for the Near East and Western Europe, respectively, comparable to the maximum rate of secular variation today, which is ∼0.3 nT/day (MacMillan and Maus, 2005). De Groot et al. (2013) estimate rates as high as 0.7 nT/day recorded in ^{14}C-dated Hawaiian basalt flows and Gomez-Paccard et al. (2012) up to 2.2 nT/day in European archeological materials. Two intensity spikes with even faster rates up to 10–15 nT/day are implied by the paleointensity values and age models of Ben-Yosef et al. (2009) and Shaar et al. (2011) for magnetite-containing slag piles from ancient copper-smelting sites in the Near East. On theoretical grounds, though, Livermore et al. (2013) argue that a rate of ∼2 nT/day is a geophysically sound upper bound, based on assumptions that radial magnetic diffusion near the CMB is negligible and that the field structure and rms fluid velocity there were not greatly different from that currently inferred for the recent field. Finally, during the very different field configuration of a polarity reversal recorded in a 15.6 Ma basaltic section in Nevada, Bogue and Glen (2010) report evidence suggesting rapid change in the transitional field direction of around 1°/wk, which implies greater than ∼20 nT/day assuming a reasonable transitional field intensity of 10 μT. Although their case bears superficial similarities to that at Steens, the rock magnetic properties and behavior are very different and so is their method, which is based on the length of time between the emplacement of a flow and its baking by the overlying flow calculated with a conductive cooling model. To sum up, despite the demise of the case for an impulsive field change of ∼300 nT/day during the Steens Mountain reversal, the question whether or not brief episodes of field change much faster than current secular variation have occurred is very much alive and debated.

Acknowledgements

NSF grant EAR-0711418 and a senior research award to RSC by the Von Humboldt Foundation supported (*i*) the sample collection and experimental work carried out at UC Santa Cruz and (*ii*) the collaborative experimental research, interpretation and writing up of results carried out in Munich and Paris, respectively. RSC thanks the LMU Department of Earth and Environmental Sciences in Munich and the IPG Laboratoire de Géomagnétism et Paléomagnétisme in Paris for their warm hospitality during several research stays and Pierre Camps, Lennart de Groot, Yves Gallet, Stuart Gilder, Joe Liddicoat and Michel Prévot for helpful suggestions after reviewing the manuscript.

Appendix A. Supplementary material

Supplementary material related to this article can be found online at http://dx.doi.org/10.1016/j.epsl.2014.05.036. These data include the Google image of the most important areas described in this article.

References

Ben-Yosef, E., Tauxe, L., Levy, T.E., Shaar, R., Ron, H., Najjar, M., 2009. Geomagnetic intensity spike recorded in high resolution slag deposit in Southern Jordan. Earth Planet. Sci. Lett. 287, 529–539.

Bogue, S., Glen, J., 2010. Very rapid geomagnetic field change recorded by the partial remagnetization of a lava flow. Geophys. Res. Lett. 37, L21308.

Camp, V.E., Ross, M.E., Duncan, R.A., Jarboe, N.A., Coe, R.S., Hanan, B.B., Johnson, J.A., 2013. The Steens Basalt: earliest lavas of the Columbia River Basalt Group. In: Reidel, S.P., Camp, V.E., Ross, M.E., Wolff, J.A., Martin, B.S., Tolan, T.L., Wells, R.E. (Eds.), The Columbia River Flood Basalt Province, pp. 87–116. Geological Society of America Special Paper 497, doi:10.1130;2013.2497(04).

Camps, P., Prévot, M., Coe, R., 1995a. Revisiting the initial sites of geomagnetic field impulses during the Steens Mountain polarity reversal. Geophys. J. Int. 123, 484–506.

Camps, P., Prévot, M., Coe, R.S., 1995b. L'hypothèse des impulsions géomagnétiques pendant un renversement du champ: confrontation des données paleomagnétiques avec un modèle de refroidissement des laves. C. R. Acad. Sci. 320, 801–809.

Camps, P., Coe, R.S., Prévot, M., 1999. Transitional geomagnetic impulse hypothesis: geomagnetic fact or rock-magnetic artifact? J. Geophys. Res. 104, 17747–17758.

Camps, P., Singer, B., Carvallo, C., Goguitchaichvili, A., Fanjat, G., Allen, B., 2011. The Kamikatsura event and the Matuyama–Brunhes reversal recorded in lavas from Tjörnes Peninsula, northern Iceland. Earth Planet. Sci. Lett. 310, 33–44.

Coe, R.S., Prévot, M., 1989. Evidence suggesting extremely rapid field variation during a geomagnetic reversal. Earth Planet. Sci. Lett. 92, 292–298.

Coe, R.S., Prévot, M., Camps, P., 1995. New evidence for extraordinarily rapid change of the geomagnetic field during a reversal. Nature 374, 687–692.

Copp, D., 2003a. Magnetic flip. In: Equinox (Channel 4, UK), 65 minutes, DOX Productions, Great Britain.

Copp, D., 2003b. Magnetic storm. In: NOVA, 55 minutes, PBS, US.

Creer, K.M., 1967. Thermal demagnetization by the continuous method. In: Collinson, D.W., Creer, K.M., Runcorn, S.K. (Eds.), Methods in Palaeomagnetism. Elsevier, Amsterdam, pp. 287–295.

Creer, K.M., Petersen, N., 1969. Thermochemical magnetization in basalts. Z. Geophys. 35, 501–516.

Creer, K.M., Petersen, N., Petherbridge, J., 1970. Partial self-reversal of remanent magnetization and anisotropy of viscous magnetization in basalts. Geophys. J. R. Astron. Soc. 21, 471–483.

de Groot, L.V., Biggin, A.J., Dekkers, M.J., Langereis, C.G., Herrero-Bervera, E., 2013. Rapid regional perturbations to the recent global geomagnetic decay revealed by a new Hawaiian record. Nat. Commun. 4.

de Groot, L.V., Dekkers, M.J., Visscher, M., ter Maat, G.W., 2014. Magnetic properties and paleointensities as function of depth in a Hawaiian lava flow. Geochem. Geophys. Geosyst. 15, 1–17. http://dx.doi.org/10.1002/2013GC005094.

Draeger, U., Prévot, M., Poidras, T., Riisager, J., 2006. Single-domain chemical, thermochemical and thermal remanences in a basaltic rock. Geophys. J. Int. 166, 12–32.

Dunlop, D.J., Özdemir, Ö., 2000. Effect of grain size and domain state on thermal demagnetization tails. Geophys. Res. Lett. 27, 1311–1314.

Fabian, K., Shcherbakov, V.P., McEnroe, S.A., 2006. Measuring the Curie temperature. Geochem. Geophys. Geosyst. 14, 949–957. http://dx.doi.org/10.1029/2012GC004440.

Gallet, Y.D., Andrea, M., Genevey, A., Pinnock, F., Le Goff, M., Matthiae, P., 2013. Archaeomagnetism at Ebla (Tell Mardikh, Syria). New data on geomagnetic field intensity variations in the Near East during the Bronze Age. J. Archaeol. Sci.. http://dx.doi.org/10.1016/j.jas.2013.11.007.

Genevey, A., Gallet, Y., Thébault, E., Jesset, S., Le Goff, M., 2013. Geomagnetic field intensity variations in Western Europe over the past 1100 years. Geochem. Geophys. Geosyst. 14, 2858–2872. http://dx.doi.org/10.1002/ggge.20165.

Gomez-Paccard, M., McIntosh, G., Chauvin, A., Beamud, E., Pavon-Carrasco, F., Thiriot, J., 2012. Archaeomagnetic and rock magnetic study of six kilns from North Africa (Tunisia and Morocco). Geophys. J. Int. 189, 169–186.

Grommé, S., Wright, T.L., Peck, D.L., 1969. Magnetic properties and oxidation of iron-titanium oxide minerals in Alae and Makaopuhi lava lakes, Hawaii. J. Geophys. Res. 74, 5277–5294.

Havard, G.N., Lewis, M., 1965. Reversed partial thermo-magnetic remanence in natural and synthetic titanomagnetites. Geophys. J. 10, 59–68.

Heller, F., Petersen, N., 1982. Self-reversal explanation for the Laschamp Olby geomagnetic-field excursion. Phys. Earth Planet. Inter. 30, 358–372.

Hoffman, K.A., 1984. Late acquisition of "primary" remanence in some fresh basalts: a cause of spurious paleomagnetic results. Geophys. Res. Lett. 11, 681–684.

Hooper, P.R., Binger, G.B., Lees, K.R., 2002. Ages of the Steens and Columbia River flood basalts and their relationship to extension-related calc-alkalic volcanism in eastern Oregon. GSA Bull. 114, 43–50.

Humphreys, D.R., 1990. Physical mechanism for reversals of the earth's magnetic field during the flood. In: Proceedings of the Second International Conference on Creationism. Creation Science Fellowship, pp. 129–142.

Jarboe, N.A., Coe, R.S., Renne, P.R., Glen, J.M.G., Mankinen, E.A., 2008. Quickly erupted volcanic sections of the Steens Basalt, Columbia River Basalt Group: secular variation, tectonic rotation, and the Steens Mountain reversal. Geochem. Geophys. Geosyst. 9, Q11010.

Jarboe, N.A., Coe, R.S., Glen, M.G., 2011. Evidence from lava flows for complex polarity transitions: the new composite Steens Mountain reversal record. Geophys. J. Int. 186, 580–602.

Krása, D., Shcherbakov, V.P., Kunzmann, T., Petersen, N., 2005. Self-reversal of remanent magnetization in basalts due to partially oxidized titanomagnetites. Geophys. J. Int. 162, 115–136.

Larson, E.E., Strangway, D.W., 1969. Magnetization of Spanish Peaks dike swarm, Colorado, and Shiprock dike, New Mexico. J. Geophys. Res. 74, 1505–1514.

Le Goff, M., Gallet, Y., 2004. A new three-axis vibrating sample magnetometer for continuous high-temperature magnetization measurements: applications to paleo- and archeo-intensity determinations. Earth Planet. Sci. Lett. 229, 31–43.

Livermore, P.W., Fournier, A., Gallet, Y., 2013. Core-flow constraints on extreme archeomagnetic intensity changes. Earth Planet. Sci. Lett. 387, 145–156. http://dx.doi.org/10.1016/j.epsl.2013.11.020.

MacMillan, S., Maus, S., 2005. International Geomagnetic Reference Field—the tenth generation. Earth Planets Space 57, 1135–1140.

Mankinen, E.A., Prévot, M., Grommé, C.S., Coe, R.S., 1985. The Steens Mountain (Oregon) geomagnetic polarity transition 1. Directional history, duration of episodes, and rock magnetism. J. Geophys. Res. 90, 10.393–10.416.

Morris, E.R., Schillinger, W., Coe, R.S., Pluhar, C.J., Jarboe, N.A., 2009. Automating the 2G superconducting rock magnetometer for single-solenoid alternating field demagnetization. Geochem. Geophys. Geosyst. 10, Q05Y05.

Nagata, T., Ozima, M., 1955. Anomalous increase in thermo-remanent magnetization of ferromagnetic minerals: magnetic interaction between different constituents in ferromagnetic minerals. J. Geomagn. Geoelectr. 7, 105–120.

Petersen, N., Eisenach, P., Bleil, U., 1979. Low temperature alteration of the magnetic minerals in ocean floor basalts. In: Talwani, M., Harrison, C.G.A., Hayes, D. (Eds.), Deep Drilling Results in the Atlantic Ocean: Ocean Crust. In: American Geophysical Union Maurice Ewing Series, vol. 2. American Geophysical Union, Washington, DC, pp. 169–209.

Petrovský, E., Kapička, A., 2006. On determination of the Curie point from thermomagnetic curves. J. Geophys. Res., Solid Earth 111, B12S27. http://dx.doi.org/10.1029/2006JB004507.

Prévot, M., Mankinen, E.A., Coe, R.S., Grommé, C.S., 1985a. The Steens Mountain (Oregon) geomagnetic polarity transition 2. Field intensity variations and discussion of reversal models. J. Geophys. Res. 90, 10,417–10,448.

Prévot, M., Mankinen, E.A., Grommé, C.S., Coe, R.S., 1985b. How the geomagnetic field vector reverses polarity. Nature 316, 230–234.

Sawyer, D.A., 2003. The Neanderthal Parallax (Book 2): Humans. TOR, Tom Doherty Associates, New York. 334 pp.

Shaar, R., Ben-Yosef, E., Ron, H., Tauxe, L., Agnon, A., Kessel, R., 2011. Geomagnetic field intensity: how high can it get? How fast can it change? Constraints from Iron Age copper slag. Earth Planet. Sci. Lett. 301, 297–306.

Thellier, E., Thellier, O., 1944. Recherches géomagnétiques sur des coulées volcaniques d'Auvergne. Ann. Géophys. 1, 37–52.

Watkins, N.D., 1965. Frequency of extrusions of some Miocene lavas in Oregon during an apparent transition of polarity of geomagnetic field. Nature 206, 801–803.